

# In Vivo Functionality of a Corneal Endothelium Transplanted by Cell-Injection Therapy in a Feline Model

Cristina Bostan,<sup>1,2</sup> Mathieu Thériault,<sup>3</sup> Karolyn J. Forget,<sup>1</sup> Christelle Doyon,<sup>1,2</sup> J. Douglas Cameron,<sup>4</sup> Stéphanie Proulx,<sup>3,5</sup> and Isabelle Brunette<sup>1,2</sup>

<sup>1</sup>Maisonneuve-Rosemont Hospital Research Center, Montreal, Quebec, Canada

<sup>2</sup>Department of Ophthalmology, University of Montreal, Montreal, Quebec, Canada

<sup>3</sup>Centre d'organogénèse expérimentale de l'Université Laval/LOEX, Québec City, Quebec, Canada, and Centre de recherche du CHU de Québec-UL, Axe Médecine régénératrice, Québec City, Quebec, Canada

<sup>4</sup>Ophthalmology and Visual Neurosciences and Laboratory Medicine and Pathology, University of Minnesota School of Medicine, Minneapolis, Minnesota, United States

<sup>5</sup>Department of Ophthalmology and ENT-Head and Neck Surgery, Université Laval, Québec City, Quebec, Canada

Correspondence: Isabelle Brunette, Department of Ophthalmology, Maisonneuve-Rosemont Hospital, 5415 boulevard de l'Assomption, Montreal, QC H1T 2M4 Canada; i.brunett@videotron.ca.

Submitted: July 6, 2015

Accepted: January 30, 2016

Citation: Bostan C, Thériault M, Forget KJ, et al. In vivo functionality of a corneal endothelium transplanted by cell-injection therapy in a feline model. *Invest Ophthalmol Vis Sci*. 2016;57:1620-1634. DOI:10.1167/iops.15-17625

**PURPOSE.** To evaluate the functionality of a corneal endothelium reconstituted by injection of corneal endothelial cells (CEC) in the anterior chamber of a feline model.

**METHODS.** We operated the right eyes of 16 animals. Eight underwent central endothelial scraping and injection with  $2 \times 10^5$  ( $n = 4$ ) or  $1 \times 10^6$  ( $n = 4$ ) feline CEC supplemented with Y-27632 and labeled with 3,3'-Diocadecyl-5,5'-Di(4-Sulfophenyl)Oxycarbocyanine (SP-DiOC18[3] or DiOC). After total endothelial scraping, two eyes were injected with  $1 \times 10^6$  labeled CEC and Y-27632. The central ( $n = 3$ ) or entire ( $n = 3$ ) endothelium was scraped in six eyes followed by Y-27632 injection without CEC. Subjects were positioned eyes down for 3 hours. Outcomes included graft transparency, pachymetry, CEC morphometry, histology, electron microscopy, and function and wound healing-related protein immunostaining.

**RESULTS.** Postoperatively, corneas grafted with  $2 \times 10^5$  CEC and centrally scraped controls displayed the best transparency and pachymetry. Corneas grafted with  $1 \times 10^6$  CEC yielded intermediate results. Entirely scraped controls remained hazy and thick. Histopathology revealed a confluent endothelial monolayer expressing sodium-potassium adenosine triphosphatase ( $\text{Na}^+/\text{K}^+$ -ATPase) and zonula occludens-1 (ZO-1) in corneas grafted with  $2 \times 10^5$  CEC and centrally scraped controls, a nonuniform endothelial multilayer without expression of functional proteins in centrally scraped corneas grafted with  $1 \times 10^6$  CEC, and a nonfunctional fibrotic endothelium in entirely scraped grafts and controls. Expression of DiOC in grafts was scarce.

**CONCLUSIONS.** Injected CEC contributed little to the incompletely functional endothelium of grafted corneas. Y-27632 injection without CEC following scraping reconstituted the healthiest endothelium. Further studies investigating the therapeutic effect of Y-27632 alone are needed to validate these conclusions.

**Keywords:** corneal endothelium, corneal transplantation, corneal endothelial cell culture, cell-injection therapy, ROCK inhibitor

Corneal endothelial diseases cause blindness due to loss of corneal transparency. They were responsible for 40% of the 66,305 corneal transplantations performed in the United States in 2013.<sup>1</sup> In several parts of the world, however, donor tissue shortage limits accessibility to this therapeutic option.<sup>2-7</sup> The relentlessly increasing demand for transplantable corneas<sup>8,9</sup> and the limitations inherent to current transplantation techniques, including postoperative endothelial cell attrition<sup>10-16</sup> and immune rejection,<sup>17,18</sup> have driven the search for alternative treatments.

Tissue engineering opens a promising avenue for generating sufficient amounts of highly cellular corneal endothelial grafts to alleviate the increasing demand.<sup>19,20</sup> It is based on the ability of human endothelial cells, normally arrested in the G<sub>1</sub> phase of the cell cycle in vivo, to proliferate in vitro with the addition of growth factors.<sup>21</sup> Tissue-engineered endothelial monolayers have been successfully grafted in animal eyes.<sup>7,22-26</sup> The choice

of a carrier for these monolayers, however, remains a challenge, because of poor biocompatibility issues, interface scarring, or the persisting need for human donor tissue for carriers consisting of stroma and/or Descemet's membrane (DM).<sup>19</sup> Endothelial cell sheets not supported by a carrier are too fragile to constitute a clinically viable option.

The injection of cultured corneal endothelial cells (CEC) into the anterior chamber offers a promising therapeutic alternative. Intracameral CEC injection is significantly less invasive than any currently used keratoplasty technique. It also shares the advantages of engineered tissues, namely, standardization of in vitro production, quality control, and graft sterility, as well as the options of autologous transplantation and production of multiple grafts from a single donor cornea. Moreover, intracameral CEC injection can be repeated if needed using the same cryopreserved cell population, thus avoiding sensitization by new donor antibodies.

Intracameral CEC injection alone after CEC depletion was proven unsuccessful for endothelial transplantation in several studies.<sup>27,28</sup> Different strategies have thus been proposed to enhance adherence of injected CEC to the DM.<sup>27-35</sup> Some groups used CEC loaded with iron particles,<sup>27,28</sup> superparamagnetic microspheres<sup>36</sup> or magnetic nanoparticles,<sup>29</sup> and an extraocular magnetic field to attract CEC to the DM, however, with an uncertain long-term safety profile. Others showed that maintenance of a prone position after injection promotes cell deposition by gravity.<sup>30-32,34</sup> A promising approach was the addition of Rho-associated kinase inhibitor (ROCKi) to stimulate migration and adherence of injected CEC.<sup>34,37,38</sup>

Most of the in vivo CEC-injection studies were performed in rabbits,<sup>27-32,34,35</sup> whose endothelial cells are known to replicate spontaneously,<sup>39</sup> while only one small-sample-size study included a primate model.<sup>34</sup> The feline model has nonreplicating endothelial cells similar to those of humans,<sup>39-41</sup> and its use for the optimization of corneal transplantation techniques is well documented.<sup>42-45</sup> It is thus an interesting model for the preclinical assessment of corneal endothelial reconstitution by intracameral CEC injection.

The goal of this study was to assess the anatomy, biocompatibility, and functionality of a corneal endothelium reconstituted by injection of allogeneic CEC in the anterior chamber of a feline endothelial deficiency model. All injected eyes received ROCK inhibitor supplementation and were positioned eyes down for 3 hours after injection.

## MATERIALS AND METHODS

All experiments were conducted in accordance with the ARVO Statement for the Use of Animals in Ophthalmic and Vision Research and with the Maisonneuve-Rosemont Hospital Committee for Animal Protection guidelines.

### Endothelial Cell Isolation, Culture, and Labeling

Descemet's membranes were peeled from feline corneas and incubated in growth medium overnight at 37°C and 8% CO<sub>2</sub>.<sup>21,46</sup> They were then incubated with EDTA 0.02% for 1 hour and passed several times through a pipette. Detached cells were seeded on FNC (Athena Enzyme Systems, Baltimore, MD, USA)-coated culture dishes in Dulbecco's modified Eagle's medium (Invitrogen, Burlington, ON, Canada) containing 10% fetal bovine serum (Hyclone, Logan, UT, USA), 5 ng/mL human epidermal growth factor (Austral Biologicals, San Ramon, CA, USA), 25 µg/mL bovine pituitary extract (Biomedical Technologies, Ward Hill, MA, USA), 25 µg/mL gentamicin sulfate (Schering Canada, Pointe Claire, QC, Canada), and 100 IU/mL penicillin G (Sigma-Aldrich Corp., St. Louis, MO, USA). Four cell populations were cultured up to second passage (Supplementary Table S1) and labeled with the fluorescent membrane tracer 3,3'-diiododecyl-5,5'-Di(4-sulfophenyl)-oxycarbocyanine, sodium salt (SP-DiOC18(3)); 2 µg/mL; Molecular Probes, Eugene, OR, USA) following manufacturer instructions.

### Endothelial Cell Preoperative Characterization

Prior to grafting, cell morphology was evaluated in vitro by phase-contrast microscopy (TS100 Eclipse; Nikon, Melville, NY, USA). Corneal endothelial cells seeded on glass coverslips were fixed (paraformaldehyde 4% for 30 minutes) for immunolabeling. Cells were first labeled with Alexa Fluor 488 phalloidin (Invitrogen) for 30 minutes, then immunostained for 1 hour with either a mouse anti-sodium-potassium adenosine triphosphatase alpha 1 (Na<sup>+</sup>/K<sup>+</sup>-ATPase  $\alpha$ 1) (Millipore, Etobicoke, ON, Canada), a polyclonal anti-zonula occludens-1 (ZO-1) (Invitrogen), a mouse anti-alpha-

smooth muscle actin ( $\alpha$ -SMA) (Dako, Burlington, ON, Canada), a goat anti-fibronectin (Santa Cruz, Dallas, TX, USA), or a mouse anti-collagen type I (Sigma-Aldrich Corp.). The secondary antibodies Alexa Fluor 594 goat anti-mouse (Invitrogen), chicken anti-goat (Invitrogen), and chicken anti-rabbit (Invitrogen) were used as secondary antibodies for 45 minutes at room temperature. Antibodies were diluted in phosphate-buffered solution containing 1% bovine albumin serum (Sigma-Aldrich Corp.). Hoechst reagent 33258 or 4',6-diamidino-2-phenylindole (DAPI) was added for cell nuclei counterstaining. Fluorescence was then observed (Axio Imager.Z2 microscope; AxioVision Rel. 4.8.2.; Carl Zeiss Canada, Toronto, ON, Canada), and the percentage of  $\alpha$ -SMA-positive cells was determined (ImageJ; U.S. National Institutes of Health, Bethesda, MD, USA).

### Population

Sixteen healthy adult animals were obtained from a certified supplier. Right eyes were assigned to surgery and left eyes were used as normal nonoperated controls. Eight animals underwent central (7-mm diameter) endothelial scraping and injection with  $2 \times 10^5$  (200 K;  $n = 4$ ) or  $1 \times 10^6$  (1 M;  $n = 4$ ) feline CEC supplemented with 100 µM or 350 µM ROCKi (Y27632; Sigma-Aldrich Corp.) in 0.2 mL. Two animals underwent total (18-mm diameter) endothelial scraping followed by intracameral injection of ROCKi and 1 M CEC in 0.2 mL. After scraping off their central ( $n = 3$ ) or entire ( $n = 3$ ) endothelium, six negative control corneas were injected with ROCKi in 0.2 mL without CEC.

### Preoperative Assessment

The preoperative ophthalmic examination included slit-lamp biomicroscopy (BQ 900; Haag-Streit, Bern, Switzerland; Sony 3CCD video camera; Sony, Park Ridge, NJ, USA), central corneal pachymetry (Ultrasound Pachymeter SP 3000; Tomey, Nagoya, Japan), intraocular pressure (IOP) measurement (Tonovet, TV01; Tiolat Oy, Helsinki, Finland), and noncontact specular microscopy (Konan Medical Inc., Nishinomiya, Hyogo, Japan) for endothelial cell count and morphometry.

### Medication

All animals were given oral prophylactic famcyclovir (125 mg daily; Famvir; PMS, Montreal, QC, Canada) for the entire study period. Topical diclofenac sodium 0.1% (twice daily; Voltaren Ophtha; Alcon, Mississauga, ON, Canada) and dexamethasone 0.1% (once daily; Maxidex ointment; Alcon), as well as oral prednisone (5 mg daily), were administered for 3 days prior to surgery.

At the beginning of the surgery, subconjunctival dexamethasone (1.2 mg/0.3 mL), tobramycin (10 mg/0.25 mL), and cefazolin (55 mg/0.25 mL) were administered. Pupillary constriction, using pilocarpine 2% (Minims; Chauvin, Kingston-Upon-Thames, UK) with or without intracameral acetylcholine 1% (Miochol-E; Bausch+Lomb; Rochester, NY, USA), was sought to minimize deposition of injected CEC on the lens.

Sodium chloride 5% (twice daily; Muro 128 ointment; Bausch+Lomb), diclofenac sodium 0.1% (three times daily), and tobramycin 0.3% with dexamethasone 0.1% (once daily; Tobradex ointment; Alcon) were administered to the operated eye for the first postoperative week and tapered over 1 month. Systemic prednisone (5 mg daily) was given for 3 days after surgery.

### Endothelial Cell Transplantation

At the time of surgery, cultured CEC were detached from the culture dish using 0.05% trypsin/0.53 mM EDTA (Corning

Cellgro, Manassas, VA, USA) and suspended in 0.2 mL balanced salt solution (BSS) supplemented with 100  $\mu$ M or 350  $\mu$ M ROCKi. The same corneal surgeon (IB) performed all interventions under general anesthesia.<sup>42</sup> The central (7-mm diameter) or entire (18-mm diameter, up to 0.5 mm from the angle) recipient endothelium was gently detached in flaps (Endothelial keratoplasty spatula; Moria, Antony, France), leaving the DM denuded and intact. Continuous irrigation with BSS ensured completeness of endothelial cell removal from the DM's surface and anterior chamber. The 2-mm limbal wound was closed (CU-1 10-0 nylon; Alcon Surgical, Fort Worth, TX, USA), and recombinant tissue plasminogen activator (75  $\mu$ g/0.3 mL; Alteplase; Genentech, San Francisco, CA, USA) was injected in the anterior chamber to accelerate fibrin resorption.<sup>47,48</sup> A 30-gauge cannula, directed toward the denuded DM and away from the angle, iris, and lens, was used to inject 0.2 mL BSS:ROCKi containing 200 K, 1 M, or no CEC. The animal was then immediately turned eyes down to allow CEC deposition on the denuded DM by gravity. This position was maintained for 3 hours under general anesthesia.

### Postoperative Follow-Up

Eyes were examined on postoperative days 1 to 4, then twice a week until euthanasia. Examination included assessment of corneal transparency, intraocular inflammation, signs of rejection, and ectopic deposition of injected CEC. A subjective 0 to 4+ scale<sup>49</sup> was used to evaluate graft transparency (0: opaque cornea; 1+: moderate opacity, no iris/lens details; 2+: mild opacity, iris/lens details still visible; 3+: slight opacity, iris/lens details easily visible; 4+: clear graft, iris details fully visible). For intraocular inflammation, anterior chamber cells and flare were quantified with a 0 to 4+ scale.<sup>50</sup> Intraocular pressure and central corneal thickness (CCT) were also measured. Sutures were removed on day 10.

Two nongrafted controls (central scraping,  $n = 1$ ; entire scraping,  $n = 1$ ) were analyzed immediately after the 3-hour eyes-down positioning period to assess the endothelial damage induced by scraping. One of the centrally scraped corneas grafted with 1 M CEC was followed for 16 days and one of the centrally scraped nongrafted controls for 7 days. All other operated eyes were followed for 1 month. Animals were then euthanized (pentobarbital sodium 3 mL/2.5–5 kg intravenously). Experimental and control eyes were enucleated and the corneal-scleral buttons, iridocorneal angle, and lenses carefully dissected. Representative portions of each cornea were distributed for vital staining, histology, and scanning and transmission electron microscopy (SEM; TEM) and immunofluorescence.

### Postoperative Endothelial Cell Density and Morphometry

Vital staining was performed with trypan blue and alizarin red S (Sigma-Aldrich Corp.).<sup>51</sup> Two nonoverlapping fields of the central cornea were photographed (SteREO Discovery V12; AxioVision Rel. 4.8.2.; Carl Zeiss Canada), and a minimum of 100 cells per field were counted for endothelial cell density and morphometry analysis (KSS-409SP software, version 2.10; Cellchek XL; KonanMedical USA, Torrance, CA, USA). The percentage of hexagonal cells was used to describe pleomorphism (differences in cell shape) and the cell area coefficient of variation to describe polyemegethism (differences in cell size).<sup>52,53</sup>

### Histopathology

Two samples per cornea, the iridocorneal angle, and the lens specimens were fixed in 10% neutral buffered formalin and

processed for SEM (6360LV; JEOL, Tokyo, Japan) and light microscopy (Axio Imager.Z2). Another sample was fixed in 2.5% glutaraldehyde and processed for TEM (H-7500; Hitachi, Tokyo, Japan).<sup>46</sup> For immunofluorescence analysis, specimens were frozen in optimal cutting temperature solution (OCT; Somagen, Edmonton, AB, Canada).<sup>26</sup> Transversal cryosections (10  $\mu$ m thick) were fixed in 100% acetone (EMD, Mississauga, ON, Canada) for 10 minutes at  $-20^{\circ}\text{C}$  and immunostained for 1 hour at room temperature with the antibodies previously described, as well as a guinea pig anti-keratins 8/18 antibody (ARP, Waltham, MA, USA). Cell nuclei were counterstained with Hoechst reagent or DAPI, and fluorescence was assessed as described previously.

## RESULTS

### CEC Characterization Prior to Transplantation

All CEC populations displayed polygonal morphology in culture (Fig. 1A). The tight junction protein ZO-1 and the cell membrane endothelial function-related protein  $\text{Na}^+/\text{K}^+$ -ATPase  $\alpha 1$  were present in all (Figs. 1B, 1C). As little as  $0.07 \pm 0.04\%$  of cells expressed the endothelial-to-mesenchymal transition marker alpha-SMA (Fig. 1D). A weak background expression of type I collagen and fibronectin was noted, which was compatible with use of FNC coating (Figs. 1E, 1F). Actin was limited to the cellular perimembrane region in all populations (Figs. 1B–F).

### Assessment of the Endothelial Damage Induced by Scraping

Analysis of the two nongrafted controls (7- and 18-mm scraping and ROCK inhibitor injection) immediately after their 3-hour eyes-down postoperative positioning period confirmed the complete removal of the endothelium and the integrity of the denuded DM (Supplementary Fig. S1).

### Postoperative Clinical Outcome

Figures 2 and 3 describe the postoperative clinical evolution. Before surgery, no epithelial defects, inflammation, or neovascularization were noticed in any of the eyes. After surgery, intraocular inflammation was minimal, with few inflammatory cells and mild flare, resolving within 1 week (Figs. 3D, 3E). Significant anterior chamber inflammation was noted in only one subject (entirely scraped cornea transplanted with 1 M CEC), with condensation of web-like fibrin filaments contracting toward the posterior corneal surface. Intracameral recombinant tissue plasminogen activator (600  $\mu$ g/0.6 mL) injected in this eye on day 7 led to complete fibrin resorption by day 8. No signs of rejection (Khodadoust line, keratic precipitates) were noted during follow-up in any of the grafts.

**Corneal Transparency.** Grafted corneas progressively cleared in the first week after surgery, however, remaining overall hazier than contralateral nonoperated controls (Figs. 2A, 2B, 2E, 2J, 3A). Corneas transplanted with 200 K CEC (Fig. 2A) and centrally scraped nongrafted controls (Fig. 2D) achieved the best transparency at 1 month, with a mean score of 3.69 and 3.75, respectively. The centrally and entirely scraped corneas grafted with 1 M CEC progressed similarly, but with lower scores (Figs. 2B, 2E). The nongrafted entirely scraped corneas never cleared postoperatively (Fig. 2F).

**Central Corneal Thickness.** Figure 3B shows the evolution of the mean CCT in operated eyes. Grafted corneas remained thicker than contralateral nonoperated controls, but

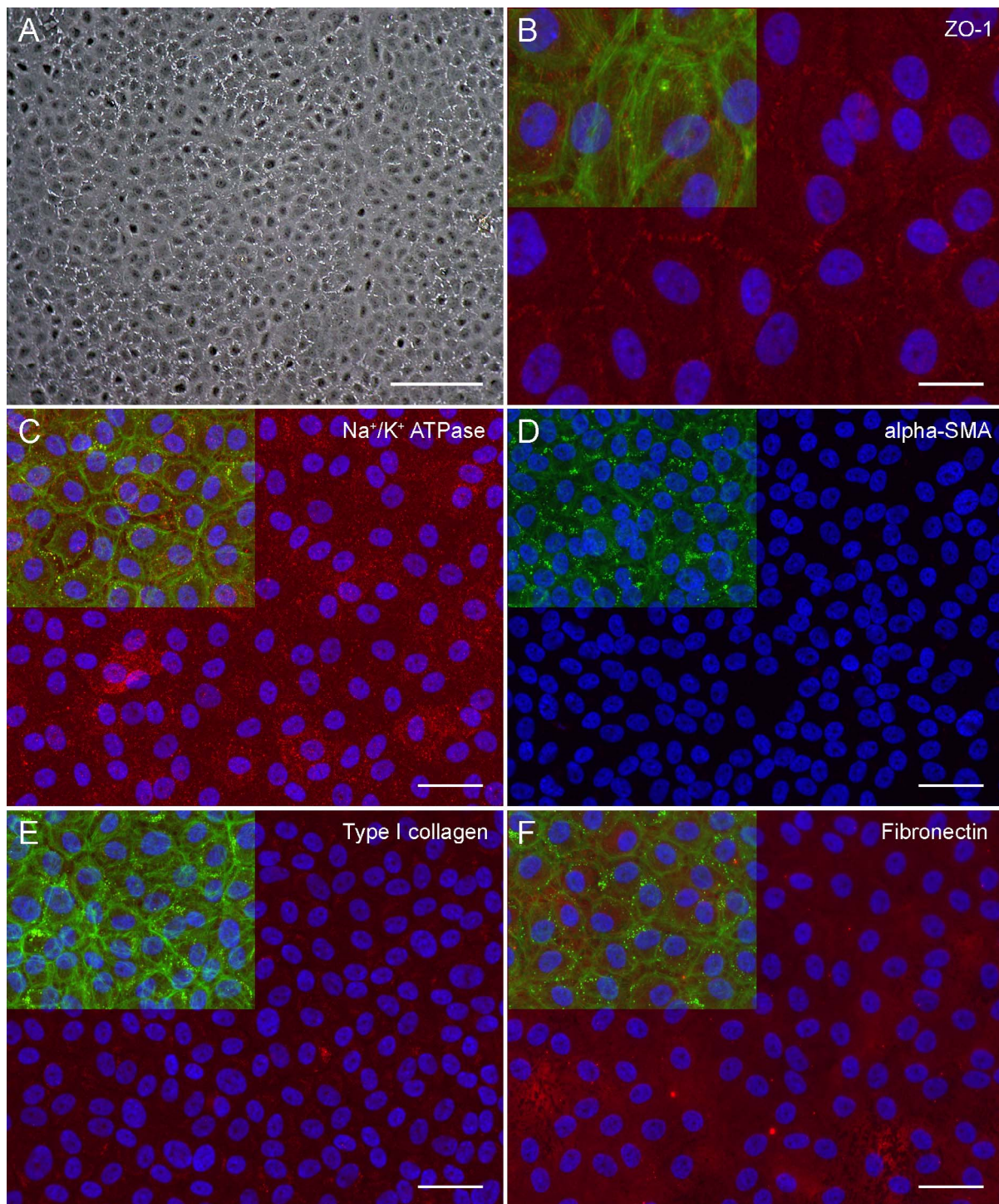


**FIGURE 1.** Corneal endothelial cells prior to grafting. (A) Cultured CEC at P2. (B–F) Immunofluorescence directed against ZO-1, Na<sup>+</sup>/K<sup>+</sup>-ATPase, α-SMA, type I collagen, or fibronectin (red) with Hoechst (blue) and phalloidin staining (green). Scale bars: 200 μm (A); 10 μm (B); 20 μm (C–F).

considerably thinner than the entirely scraped nongrafted controls, which stayed edematous and maintained CCT values above 2000 μm. Corneas grafted with 200 K CEC and the centrally scraped nongrafted controls thinned progressively, reaching mean CCT of 789 and 671 μm, respectively. Those transplanted with 1 M CEC remained relatively stable, with a mean CCT of 1248 μm at 1 month.

**Intraocular Pressure.** No significant IOP elevation was noted in any of the operated eyes (Fig. 3C).

**Posterior Corneal Haze.** On postoperative day 1, a highly reflective layer was noted at the posterior aspect of corneas injected with CEC (Figs. 2C, 2D, 2G). This haze was limited to and did not extend beyond the areas that had been scraped and grafted. With time, it lost uniformity and adopted a patchy aspect. No haze was seen in scraped but noninjected eyes, although the significant edema noted in entirely scraped nongrafted corneas might have prevented its visualization (Figs. 2H–K).

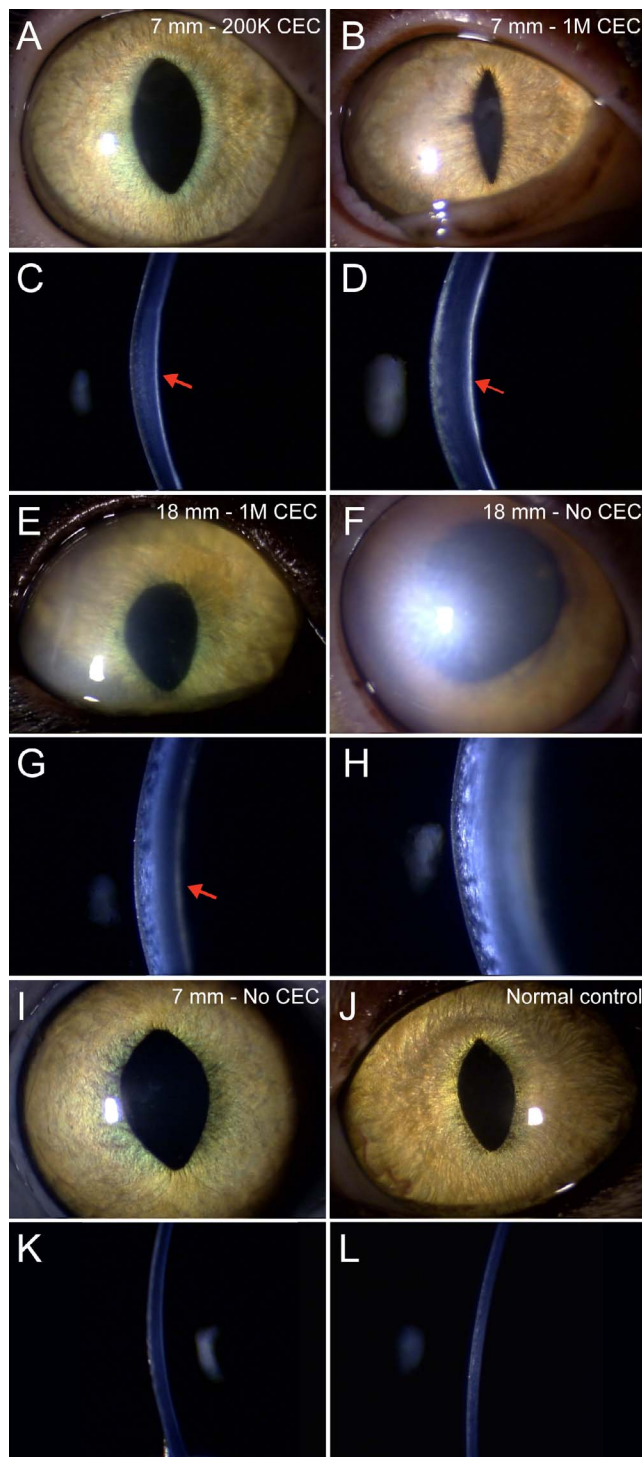


**FIGURE 2.** Operated eyes 1 month after surgery. (A, C) Centrally scraped cornea grafted with 200 K CEC. (B, D) Centrally scraped cornea grafted with 1 M CEC. (E, G) Entirely scraped cornea grafted with 1 M CEC. A condensed, highly reflective layer is visible at the posterior aspect of all grafts (*arrows*). (F, H) Nongrafted entirely scraped cornea. Considerable stromal and subepithelial edema can be noted. (I, K) Nongrafted centrally scraped cornea. (J, L) Normal nonoperated control.

### Endothelial Cell Density and Morphometry

Endothelial cell counts and morphology findings are summarized in the Table and illustrated in Figure 4. Specular microscopy showed a normal corneal endothelium in all eyes

prior to surgery. One month after surgery, all operated eyes had lower cell counts than contralateral nonoperated controls. Centrally scraped nongrafted controls (Fig. 4E) and corneas grafted with 200 K CEC (Fig. 4A) displayed the greatest cell densities, followed by centrally (Fig. 4B) and entirely scraped (Fig. 4C) corneas grafted with 1 M CEC. No cells were seen in the center of the entirely scraped nongrafted controls (Fig. 4D). All repopulated regions displayed polymegethism (greater mean coefficients of variation in cell area) and pleomorphism (loss of hexagonality).

### Scanning Electron Microscopy

Overall, SEM corroborated vital staining findings. Confluent polygonal cells covered the surface of centrally scraped corneas grafted with 200 K, 1 M, or no CEC (Figs. 5A–C, 5G). Cells were smaller and more uniformly arranged in centrally scraped nongrafted controls (Fig. 5G). Interestingly, arciform patterns were noted in centrally scraped corneas grafted with 1 M CEC, corresponding to areas of redundant plasma membrane at the cell periphery and suggesting the presence of cells underneath the superficial layer (Figs. 5B, 5C). The large, irregular, stretched cells noted in the entirely scraped corneas grafted with 1 M CEC (Figs. 5D, 5E) displayed hypertrophic intercellular junctions, with abundant interdigitating cytoplasmic projections extending toward neighboring cells. Patches of disorganized fibrillar material and rare fibroblastic-like cells were seen in entirely scraped nongrafted controls (Fig. 5F).

### Light Microscopy Cross Sections

A monolayer of cells covered the DM in centrally scraped corneas grafted with 200 K CEC and in centrally scraped nongrafted corneas (Figs. 6A, 6E). A multilayer was noted on the posterior aspect of the DM in all eyes grafted with 1 M CEC and in entirely scraped nongrafted controls (Figs. 6B–D). One of the corneas grafted with 200 K CEC displayed a similar multilayer.

### Transmission Electron Microscopy

The centrally scraped corneas grafted with 200 K CEC (Figs. 7A–D) were repopulated by a monolayer of either attenuated endothelial cells with few intracytoplasmic organelles and no prominent endoplasmic reticulum (Figs. 7A, 7B) or healthy-appearing cells with well-defined intercellular junctions (Figs. 7C, 7D). Some subendothelial extracellular matrix was present (asterisk). Beyond the centrally scraped area, recipient cells looked healthy and active (Fig. 7F), and were well attached to the DM, without abnormal extracellular matrix. Their healthy appearance ruled out a more general toxic injury to anterior chamber structures that could have occurred at the time of surgery.

Centrally scraped corneas grafted with 1 M CEC (Figs. 7G–I) yielded variable results, ranging from a monolayer (Fig. 7G), similar to that obtained in corneas grafted with 200 K CEC, to a multilayer (Fig. 7H) consisting of two to four layers of tightly packed rounded cells, connected by junctional complexes (Fig. 7I), and stacked without polarity. This multilayered structure was consistent with the arciform patterns seen in SEM. The cells looked active and healthy, with a large nucleus, chromatin margination, mitochondria, lysosomes, and endoplasmic reticulum in all layers. Subendothelial deposition of fibrillar material was noted.

The entirely scraped corneas injected with 1 M CEC (Figs. 7J–L) were covered by an abundant extracellular matrix deposited in multiple successive wavy layers and composed of disorganized fibrils (Fig. 7K). Thin spindle-shaped fibroblas-

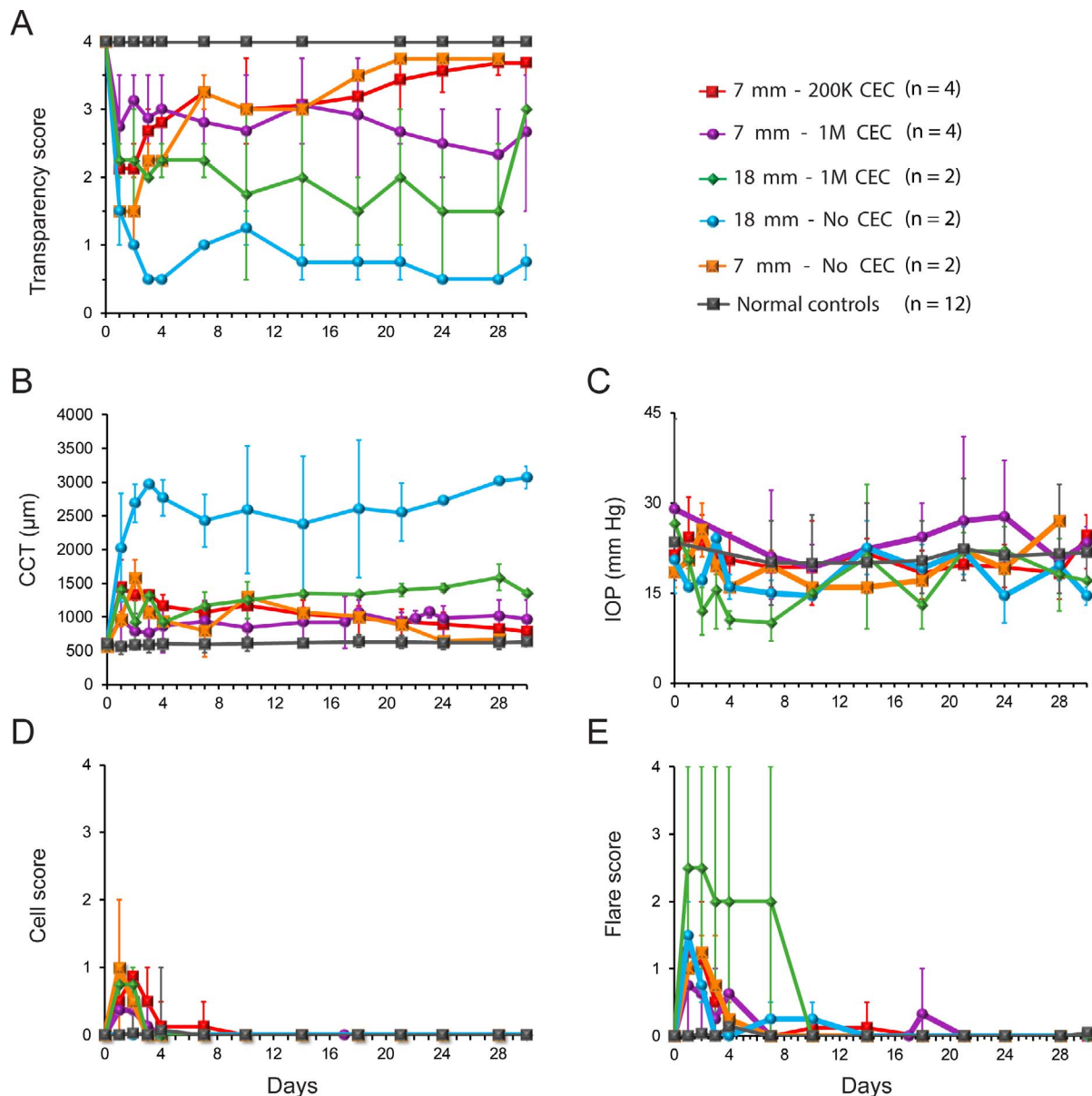


FIGURE 3. Clinical evolution of the operated eyes. (A) Transparency score. (B) Central corneal thickness. (C) Intraocular pressure. (D) Anterior chamber inflammatory cell score. (E) Anterior chamber flare score. Minimum and maximum values around means are presented.

tic-like cells, with lost polarity, were interspersed within these layers, without apparent intercellular contact (Fig. 7L). Most of these cells appeared attenuated or showed signs of degeneration, such as large intracytoplasmic vacuoles and mitochondria with amplified cristae. A thin superficial layer of confluent stretched cells was noted on top of this fibrous membrane (Fig. 7J), consistent with the cell sheet observed in SEM. One of the corneas grafted with 200 K CEC displayed a similar fibrotic multilayer (Fig. 7E).

The entirely scraped nongrafted corneas (Fig. 7M) also yielded a thick multilayered membrane with scarce elongated fibroblastic-like cells. This membrane, however, was thinner and with fewer cells than after injection of 1 M CEC. Endothelial cells were seen in the extreme periphery, near the limbus, which was compatible with the surgical technique used to remove the endothelium (Fig. 7N).

Centrally scraped nongrafted controls displayed a regular monolayer of healthy-looking cells, with normal ultrastructure

and no extracellular fibrillar accumulation (Figs. 7O, 7P). The DM was undamaged and unremarkable in all specimens.

### Immunofluorescence

All specimens were positive for keratin 8/18 (Fig. 8, column 1), a protein normally expressed by CEC.<sup>54</sup> The tight junction-associated protein ZO-1 and the Na<sup>+</sup>/K<sup>+</sup>-ATPase  $\alpha$ 1 protein were adequately expressed only in centrally scraped corneas grafted with 200 K CEC and in centrally scraped nongrafted controls (Fig. 8, columns 2, 3). Confocal microscopy confirmed that ZO-1 in these specimens, as in normal controls, was localized at the apical aspect of the lateral cell membrane. Specimens displaying a multilayered endothelium in light microscopy were positive for  $\alpha$ -SMA, type I collagen, and fibronectin (Fig. 9, rows 2–4);  $\alpha$ -SMA and fibronectin were also expressed in one of the centrally scraped nongrafted corneas at 7 days (Fig. 9, row 5). Expression of DiOC

TABLE. Endothelial Cell Counts and Morphology

	7 mm, 200 K CEC, <i>n</i> = 4	7 mm, 1 M CEC, <i>n</i> = 4	18 mm, 1 M CEC, <i>n</i> = 2	18 mm, No CEC, <i>n</i> = 2	7 mm, No CEC, <i>n</i> = 2	Nonoperated Controls, <i>n</i> = 12
Cell count, cells/mm <sup>2</sup>	1015 (673, 1295)	715 (511, 870)	681 (462, 900)	0 (0, 0)	1113 (785, 1442)	3271 (2321, 3986)
Cell area, μm <sup>2</sup>	1059 (774, 1487)	1479 (1389, 1164)	1718 (1271, 2165)	N/A	985 (695, 1275)	312 (251, 431)
CV of cell area	48 (42, 53)	48 (36, 60)	45 (43, 47)	N/A	46 (36, 55)	23 (18, 29)
6-sided cells, %	47 (46, 50)	44 (37, 47)	45 (35, 55)	N/A	47 (42, 52)	70 (60, 76)

CV, coefficient of variation.

\* Averages (min, max) are reported. N/A, not applicable.

was nonexistent in grafted corneas displaying an endothelial monolayer, but present, although scant, in multilayered grafts (Figs. 8, 9, rows 1–3). No DiOC was noted in scraped but noninjected corneas and normal controls (Figs. 8, 9, rows 4–6).

### Ectopic Deposition of Injected CEC

Immediately after injection, discrete CEC deposits were observed at the slit-lamp on the recipient endothelium, just outside the scraped area (Supplementary Fig. S2A), but were

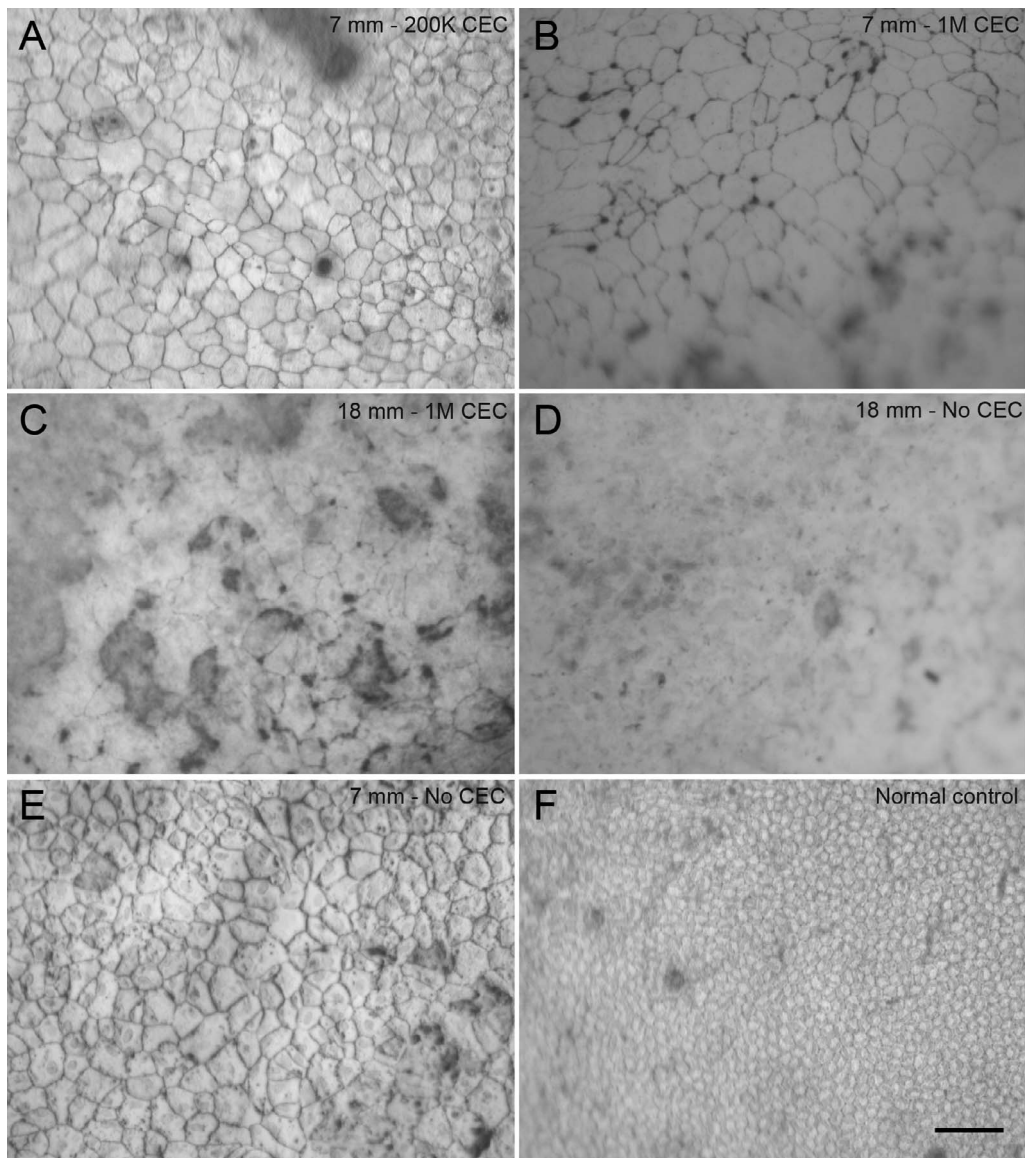
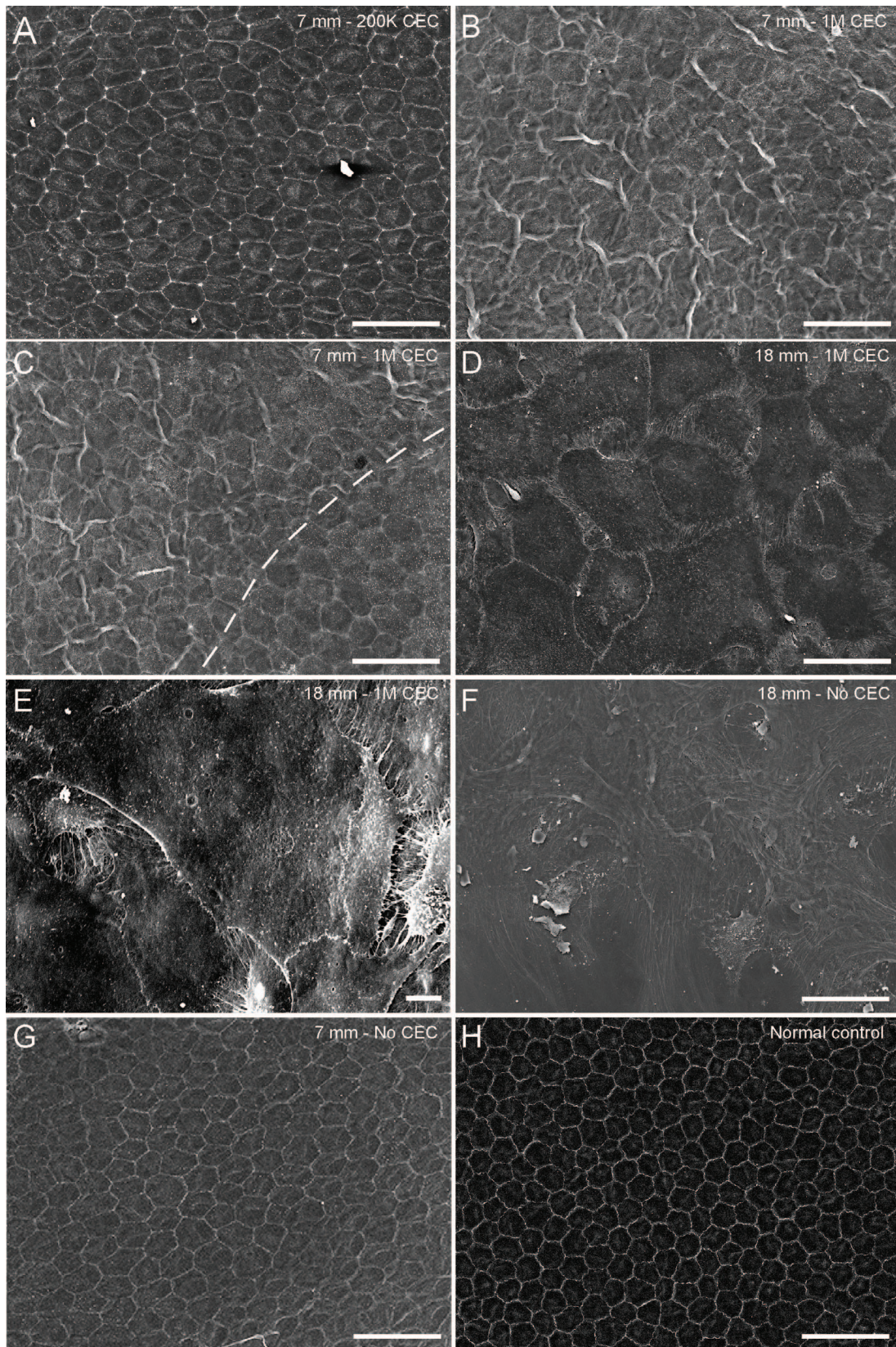
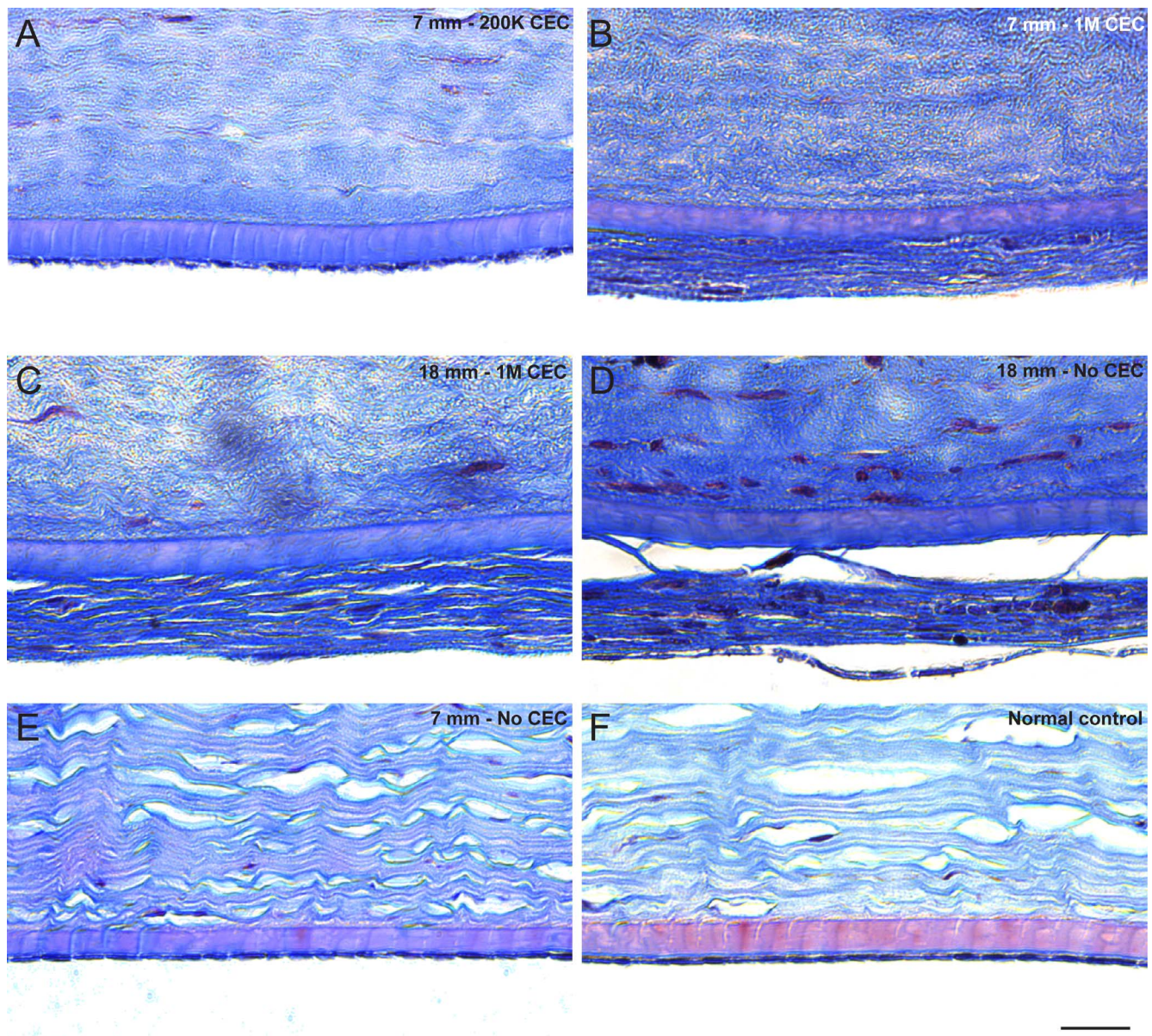


FIGURE 4. Alizarin red and trypan blue vital staining. (A) Centrally scraped cornea grafted with 200 K CEC. (B) Centrally scraped cornea grafted with 1 M CEC. (C) Entirely scraped cornea grafted with 1 M CEC. (D) Nongrafted entirely scraped cornea. (E) Nongrafted centrally scraped cornea. (F) Normal nonoperated control. Scale bar: 100 μm.



**FIGURE 5.** SEM. (A) Centrally scraped cornea grafted with 200 K CEC. (B, C) Centrally scraped cornea grafted with 1 M CEC. Arciform patterns suggesting overlapping cells are visible in the central region (B), but disappear beyond the junction with the recipient endothelium (*dashed line*) (C). (D, E) Entirely scraped cornea grafted with 1 M CEC. Hypertrophic junctions (D) with abundant cytoplasmic projections (E) between large, irregularly shaped cells are visible. (F) Nongrafted entirely scraped cornea. (G) Nongrafted centrally scraped cornea. (H) Normal nonoperated control. *Scale bars:* 10 μm.





**FIGURE 6.** Histology. (A) Centrally scraped cornea grafted with 200 K CEC. (B) Centrally scraped cornea grafted with 1 M CEC. (C) Entirely scraped cornea grafted with 1 M CEC. (D) Nongrafted entirely scraped cornea. (E) Nongrafted centrally scraped cornea. (F) Normal nonoperated control. (A, E, F) The DM is covered by a cellular monolayer. (B–D) A multilayered membrane is present on the posterior aspect of the DM. Scale bar: 10  $\mu$ m.

no longer visible after the first week. Small aggregates were also noted on the anterior lens capsule in all injected eyes, progressively flattening and fading with time (Supplementary Fig. S2B). At 1 month after surgery, no such deposits were visible on the anterior lens capsule or in the trabeculum of grafted eyes in histology sections (Supplementary Figs. S2C, S2D). No deposits or membrane was noticed on the iris at the slit-lamp.

## DISCUSSION

In this paper, we report on the structural and functional characteristics of a corneal endothelium reconstituted by injection of allogeneic CEC in the anterior chamber of a feline model, whose endothelial cells, as in humans, do not replicate *in vivo*.<sup>39,42</sup>

## Minimal Invasiveness of Cell-Injection Therapy

Intracameral CEC injection proved to be minimally invasive, generating only little postoperative inflammation. There were no signs of rejection. Trabecular obstruction by injected CEC, if any, was transient and negligible, with no postoperative IOP elevation, similar to what has been reported in the literature.<sup>27,28,34</sup> Corneal endothelial cell deposits on other anterior chamber structures have not been described in previous studies. The deposits on the peripheral recipient endothelium faded away after 1 week and were not noted in TEM and immunofluorescence at 1 month, suggesting that they detached with time and were washed out through the trabeculum. The absence of CEC deposits on the anterior capsule in histology at 1 month indicates that they gradually detached as well. However, given the possibility of visual axis obstruction, these deposits require further evaluation.

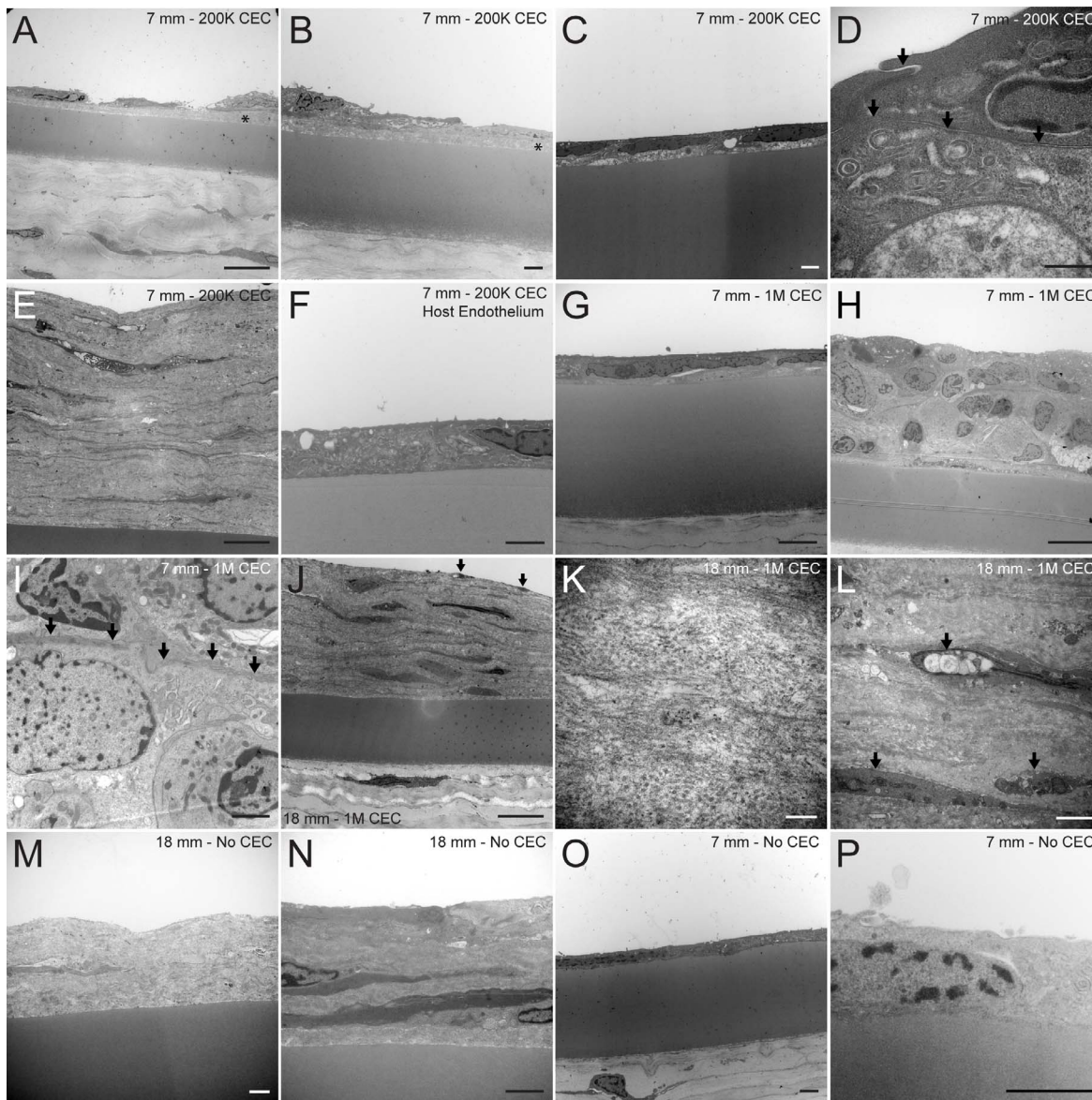


**FIGURE 7.** TEM. (A–F) Centrally scraped cornea transplanted with 200 K CEC. (A, B) Attenuated endothelial monolayer, with no intercellular junctions, separated from the DM by subendothelial fibrillar material (*asterisk*). (C) Healthy-appearing endothelial monolayer with (D) well-defined intercellular junctions (*arrows*). (E) Multilayered fibrotic endothelium in one of the centrally scraped corneas grafted with 200 K CEC. (F) Normal peripheral host endothelium. (G–I) Centrally scraped cornea grafted with 1 M CEC. Variable endothelial thickness was noted, ranging from a monolayer (G) to a multilayer (H). (I) Interdigitations between cells stacked in multilayers (*arrows*). (J–L) Entirely scraped cornea transplanted with 1 M CEC. (J) Fibroblastic-like cells interspersed within an abundant extracellular matrix and superficial layer of attenuated cells on top (*arrows*). (K) Fibrils are perpendicular and parallel to DM. (L) Cells show signs of degeneration (*arrows*). (M, N) Entirely scraped nongrafted cornea. (M) Abundant fibrotic extracellular matrix in the scraped region. (N) Remaining recipient cells in the far periphery near the angle. (O, P) Centrally scraped nongrafted cornea with a normal endothelial monolayer. Scale bars: 10  $\mu\text{m}$  (A, E, H, J); 2  $\mu\text{m}$  (B, C, F, G, I, L–P); 0.5  $\mu\text{m}$  (D); 0.1  $\mu\text{m}$  (K).

### Incomplete Functionality of the New Corneal Endothelium

In all grafts, the performance of the new corneal endothelium was superior to that of entirely scraped nongrafted corneas but inferior to that of an intact endothelium, indicating incomplete functionality.

The hypothesis that the injection of a larger number of CEC would result in better clinical outcomes was not confirmed. While 200 K CEC is sufficient to repopulate a 7-mm denuded surface in controlled cell culture conditions, their adherence to the DM might be limited by factors associated with the *in vivo* environment that are more difficult to control, such as head

and eye movement, intracameral aqueous flow, and low degrees of intraocular inflammation. Since injection of 200 K CEC yielded an incompletely functional endothelium, we hypothesized that injecting more CEC (1 M) would lead to the adherence of greater CEC numbers to the DM and, thus, better clinical and histopathologic outcomes. However, results showed that centrally scraped corneas grafted with 200 K CEC were clearer and thinner than those grafted with 1 M CEC. Despite signs of ultrastructural instability, their new endothelial monolayer displayed greater cell densities and expressed the function-related proteins ZO-1 and  $\text{Na}^+/\text{K}^+\text{-ATPase}$ , which were not observed in the multilayered endothelium of centrally scraped corneas grafted with 1 M CEC.

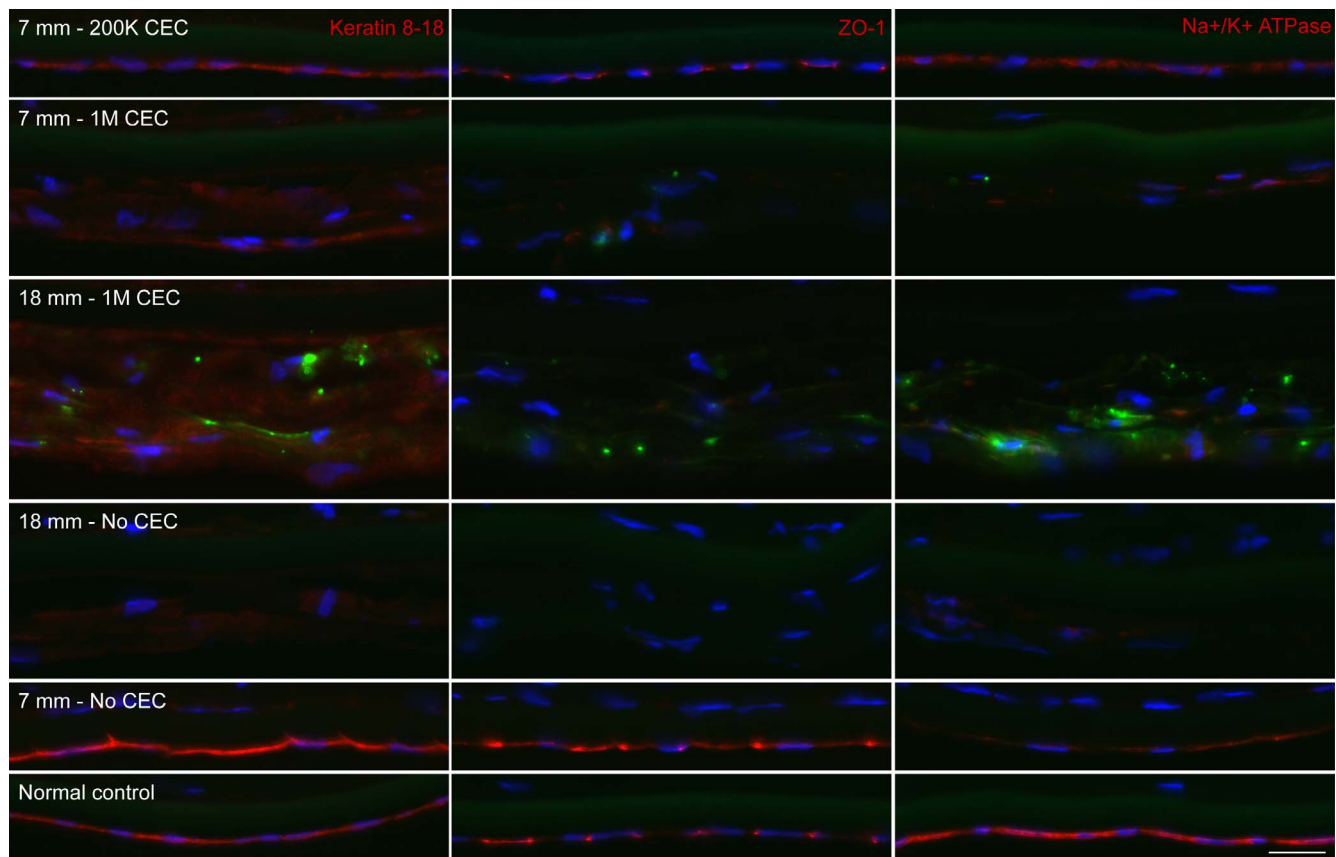


**FIGURE 8.** Immunofluorescence staining (red) of endothelial cell marker K8/18 (column 1) and functional proteins ZO-1 (column 2) and Na<sup>+</sup>/K<sup>+</sup>-ATPase  $\alpha$ 1 (column 3). Row 1: centrally scraped cornea grafted with 200 K CEC. Row 2: centrally scraped cornea grafted with 1 M CEC. Row 3: entirely scraped cornea grafted with 1 M CEC. Row 4: nongrafted entirely scraped cornea. Row 5: Nongrafted centrally scraped cornea. Row 6: normal nonoperated control. Cell nuclei counterstaining with Hoescht (blue). DiOC labeling (green). Scale bar: 10  $\mu$ m.

Okumura and colleagues<sup>34</sup> injected 200 K CEC with or without ROCK inhibitor supplementation in entirely scraped rabbit and monkey eyes followed by 3-hour eyes-down positioning. Primate corneas, which have nonreplicating CEC similar to those of felines, recovered transparency, thickness, and expression of functional endothelial proteins following injection of 200 K ROCK inhibitor-supplemented CEC, similar to our centrally scraped corneas grafted with 200 K CEC.

Given the functional endothelial monolayer reconstituted in centrally scraped nongrafted controls in our study, it appears that endothelial scraping alone without CEC injection provided its therapeutic effect through migration of peripheral recipient endothelial cells over the denuded DM. The persistent corneal edema and the fibrotic healing response observed in entirely scraped nongrafted controls suggest, however, that a critical number of remaining host endothelial cells are needed to enable effective repopulation of the scraped region.

### Contribution of Injected CEC to the New Endothelium

Unlike what was seen in previous studies in which the injected CEC were similarly labeled with a fluorescent cell tracker,<sup>27,28,30–32,34</sup> DiOC expression in our grafts was scarce to nonexistent. Corneas grafted with 200 K CEC and displaying an endothelial monolayer did not express DiOC, while multilayers of corneas grafted with 1 M CEC expressed it only sparsely.

Photobleaching of the fluorescent tracker with time or its release from injected CEC could explain DiOC scarcity in our specimens. However, repopulation of the central denuded DM by recipient CEC from peripheral unscraped regions, with limited contribution of injected CEC, is more probable.

Rho guanosine phosphatases (Rho GTPases) and their downstream effectors, Rho-associated kinases (ROCK), play a critical role in cell motility, adhesion, and progression through the cell cycle via modulation of the intracellular cytoskeleton.<sup>55</sup> Downregulation of this pathway with a selective ROCK inhibitor, Y27632, has been explored in vitro and in vivo on rabbit, monkey, bovine, and human CEC.<sup>34,37,38,56–61</sup> Its effects included enhancement of cell adhesion to substrate, migration, proliferation, and wound healing, as well as suppression of apoptosis. Okumura and colleagues<sup>34</sup> showed that ROCK inhibitor supplementation for CEC-injection therapy in the primate aids the recovery of a more functional new endothelium. However, since the contribution of injected CEC to the new endothelium in the primate is unknown, it is unclear whether the ROCK inhibitor treatment effect was mediated through increased adherence of injected CEC, stimulated migration of peripheral recipient endothelial cells, or both.

### Fibrotic Healing Response

Multilayering of the endothelium was noted in corneas grafted with 1 M CEC, in one of the centrally scraped corneas grafted with 200 K CEC, and in entirely scraped controls. It coincided with the expression of type I collagen, fibronectin, and  $\alpha$ -SMA, suggesting transition to a myofibroblastic phenotype. Mesen-

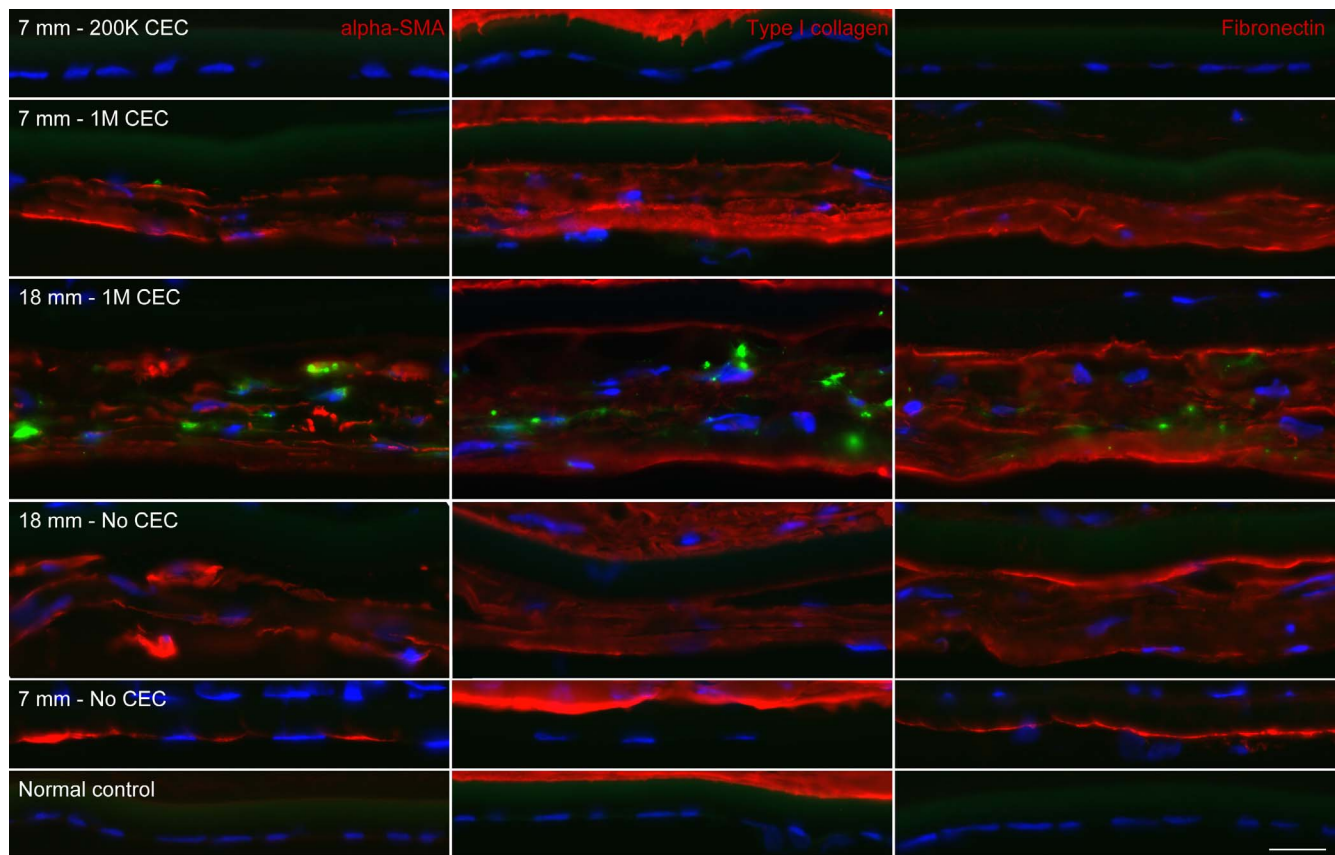


**FIGURE 9.** Immunofluorescence staining (red) of  $\alpha$ -SMA (column 1), type I collagen (column 2), and fibronectin (column 3). Row 1: Centrally scraped cornea grafted with 200 K CEC and 100  $\mu$ M ROCKi. Row 2: centrally scraped cornea grafted with 1 M CEC and 100  $\mu$ M ROCKi. Row 3: entirely scraped cornea grafted with 1 M CEC. Row 4: nongrafted entirely scraped cornea. Row 5: nongrafted centrally scraped cornea. Row 6: normal nonoperated control. Cell nuclei counterstaining with Hoescht (blue). DiOC labeling (green). Scale bar: 10  $\mu$ m.

chymally transited CEC have been shown to secrete type I collagen, instead of normally produced basement membrane type IV collagen,<sup>62,63</sup> and fibronectin.<sup>63–65</sup> Alpha-SMA is also a marker of mesenchymal transition,<sup>66,67</sup> and its presence has been attributed to pathologic healing states, such as pseudo-phakic bullous keratopathy in humans,<sup>68</sup> after alkali injury in rabbit corneas,<sup>69</sup> or after transcorneal freezing in the feline.<sup>64</sup> Importantly, our preoperative assessment showed that injected CEC did not express  $\alpha$ -SMA and displayed normal morphology, reducing the possibility of transplanting already mesenchymally transited cells. It should be emphasized that cross-sectional histopathology assessment of the new endothelium is essential to document multilayering or formation of a retrocorneal fibrous membrane.

Corneal endothelial multilayering in association with myofibroblastic transformation, loss of cell-to-cell connectivity, and increased proliferation has been reported during wound healing after transcorneal freezing in the rabbit and feline models.<sup>39,62–64,70</sup> This healing mechanism was opposed to that following endothelial scraping injuries of less than 4 mm, which involved preservation of endothelial differentiation and cell-to-cell junctions.<sup>52,62,71–73</sup> In our study, after scraping over a 7-mm diameter with no CEC injection, the recipient endothelial cells spread and enlarged to cover the deficit, resulting in a confluent monolayer with preservation of endothelial differentiation and cell-to-cell junctions, similar to observations reported in the literature following smaller scrape injuries.<sup>52,62,71–73</sup> On the other hand, healing of 18-mm-diameter injuries, with or without CEC injection, induced a fibrotic response resembling that triggered by transcorneal

freezing. These results are consistent with the literature in suggesting that endothelial wound healing is influenced by the size and nature of the damage, a variable that should be kept in mind when investigating wound healing after CEC injection.

The fibroblastic-like cells interspersed within the retrocorneal fibrous membrane observed in our entirely scraped corneas could have originated from different sources. Stromal keratocyte downgrowth through breaks in the DM<sup>74–76</sup> is unlikely, since special care was taken to leave the DM intact at the time of surgery, with confirmation of its integrity by TEM. Significant contribution of circulating inflammatory cells<sup>70,75</sup> is also unlikely, since anterior chamber inflammation was minimal. The improbable implication of stromal and inflammatory cells is further supported by the expression of the corneal endothelial marker K8/18 in all specimens with fibrous multilayering, pointing toward CEC as the most plausible source. Retrocorneal fibrous membranes composed of mesenchymally transited fibroblastic-like endothelial cells and similar to the membranes noted herein have been previously described.<sup>62–64,70,77–79</sup> In this study, since they formed in scraped corneas both injected and not with CEC, host CEC having migrated from the far periphery were likely the main source, although donor CEC contribution to the fibrotic reaction cannot be excluded.

In conclusion, allogeneic CEC-injection therapy with ROCK inhibitor supplementation and eyes-down positioning in the feline reconstituted an incompletely functional corneal endothelium. The new endothelium in corneas grafted with 200 K CEC displayed functionality and anatomical integrity superior to that of corneas grafted with 1 M CEC, but remained inferior

to normal controls. Scarcity of DiOC in all grafted corneas suggested a limited contribution of injected CEC to the new endothelium, reconstituted mainly by migration of remaining recipient cells. Endothelial scraping without CEC injection allowed the reconstitution of the healthiest endothelium, provided that sufficient peripheral host endothelial cells were left intact. These findings question the utility of CEC-injection therapy for the treatment of endothelial deficiency. Given the recently reported promising outcomes with ROCK inhibitor eye drops in the rabbit model,<sup>80</sup> it is possible that scraping and ROCK inhibitor treatment alone is sufficient to reconstitute a functional endothelium through a wound healing-stimulating mechanism. Further studies investigating the therapeutic effect of ROCK inhibitor without CEC injection on the healing of an endothelial deficit are warranted in order to validate these conclusions.

### Acknowledgments

The authors thank Myriam Barcille, Xinling Liu, Steve Breault, André Deveault, Benjamin Goyer, Angèle Halley, Delphine Mathieu, Catherine Mauger-Labelle, Natalie Tessier, Nour Haydari, Marie-Claude Perron, Eugen Lungu, Caroline Audet, Jeanne d'Arc Uwamaliya, and Élodie Samson, as well as the LOEX histology and the IBIS electron microscopy research assistants for their technical and/or intellectual support.

Supported by The Canadian Institutes for Health Research, Ontario, Canada; the FRQ-S Vision Health Research Network and the FRQ-S ThéCell Network, Montreal, QC, Canada. CB holds a Master's Training for Medical Students FRQ-S Award. MT holds a Doctoral Training Excellence Award for Research in Vision from Centre LOEX of Université Laval, Quebec, Canada. JDC is supported in part by an unrestricted grant from Research to Prevent Blindness to the Department of Ophthalmology and Visual Neuroscience of University of Minnesota. SP is an FRQ-S Research Scholar Junior 1. IB is the recipient of the Charles-Albert Poissant Research Chair in Corneal Transplantation, University of Montreal, Quebec, Canada. Funding organizations had no role in the design or conduct of this study.

Disclosure: C. Bostan, None; M. Thériault, None; K.J. Forget, None; C. Doyon, None; J.D. Cameron, None; S. Proulx, None; I. Brunette, None

### References

- 2013 Eye Banking Statistical Report. Washington, DC: Eye Bank Association of America; 2014:1-114.
- Cao KY, Dorrepaal SJ, Seamone C, Slomovic AR. Demographics of corneal transplantation in Canada in 2004. *Can J Ophthalmol*. 2006;41:688-692.
- Poinard C, Tuppin P, Loty B, Delbosc B. The French national waiting list for keratoplasty created in 1999: patient registration, indications, characteristics, and turnover [in French]. *J Fr Ophtalmol*. 2003;26:911-919.
- Rasouli M, Caraiscos VB, Slomovic AR. Efficacy of Routine Notification and Request on reducing corneal transplantation wait times in Canada. *Can J Ophthalmol*. 2009;44:31-35.
- Reinhard T, Bohringer D, Bogen A, Sundmacher R. The transplantation law: a chance to overcome the shortage of corneal grafts in Germany? *Transplant Proc*. 2002;34:1322-1324.
- Sony P, Sharma N, Sen S, Vajpayee RB. Indications of penetrating keratoplasty in northern India. *Cornea*. 2005;24:989-991.
- Sumide T, Nishida K, Yamato M, et al. Functional human corneal endothelial cell sheets harvested from temperature-responsive culture surfaces. *FASEB J*. 2006;20:392-394.
- Tan DT, Dart JK, Holland EJ, Kinoshita S. Corneal transplantation. *Lancet*. 2012;379:1749-1761.
- Chu W. The past twenty-five years in eye banking. *Cornea*. 2000;19:754-765.
- Bohringer D, Bohringer S, Poxleitner K, et al. Long-term graft survival in penetrating keratoplasty: the biexponential model of chronic endothelial cell loss revisited. *Cornea*. 2010;29:1113-1117.
- Guerra FP, Anshu A, Price MO, Giebel AW, Price FW. Descemet's membrane endothelial keratoplasty: prospective study of 1-year visual outcomes, graft survival, and endothelial cell loss. *Ophthalmology*. 2011;118:2368-2373.
- Lass JH, Sugar A, Benetz BA, et al. Endothelial cell density to predict endothelial graft failure after penetrating keratoplasty. *Arch Ophthalmol*. 2010;128:63-69.
- Patel SV, Hodge DO, Bourne WM. Corneal endothelium and postoperative outcomes 15 years after penetrating keratoplasty. *Am J Ophthalmol*. 2005;139:311-319.
- Price MO, Price FW Jr. Endothelial cell loss after descemet stripping with endothelial keratoplasty influencing factors and 2-year trend. *Ophthalmology*. 2008;115:857-865.
- Terry MA, Chen ES, Shamie N, Hoar KL, Friend DJ. Endothelial cell loss after Descemet's stripping endothelial keratoplasty in a large prospective series. *Ophthalmology*. 2008;115:488-496, e483.
- Tourtas T, Laaser K, Bachmann BO, Cursiefen C, Kruse FE. Descemet membrane endothelial keratoplasty versus descemet stripping automated endothelial keratoplasty. *Am J Ophthalmol*. 2012;153:1082-1090, e1082.
- Anshu A, Price MO, Price FW Jr. Risk of corneal transplant rejection significantly reduced with Descemet's membrane endothelial keratoplasty. *Ophthalmology*. 2012;119:536-540.
- Price MO, Jordan CS, Moore G, Price FW Jr. Graft rejection episodes after Descemet stripping with endothelial keratoplasty: part two: the statistical analysis of probability and risk factors. *Br J Ophthalmol*. 2009;93:391-395.
- Proulx S, Brunette I. Methods being developed for preparation, delivery and transplantation of a tissue-engineered corneal endothelium. *Exp Eye Res*. 2012;95:68-75.
- Tan TE, Peh GS, George BL, et al. A cost-minimization analysis of tissue-engineered constructs for corneal endothelial transplantation. *PLoS One*. 2014;9:e100563.
- Joyce NC, Zhu CC. Human corneal endothelial cell proliferation: potential for use in regenerative medicine. *Cornea*. 2004;23:S8-S19.
- Hitani K, Yokoo S, Honda N, Usui T, Yamagami S, Amano S. Transplantation of a sheet of human corneal endothelial cell in a rabbit model. *Mol Vis*. 2008;14:1-9.
- Koizumi N, Sakamoto Y, Okumura N, et al. Cultivated corneal endothelial cell sheet transplantation in a primate model. *Invest Ophthalmol Vis Sci*. 2007;48:4519-4526.
- Lai JY, Chen KH, Hsiue GH. Tissue-engineered human corneal endothelial cell sheet transplantation in a rabbit model using functional biomaterials. *Transplantation*. 2007;84:1222-1232.
- Mimura T, Amano S, Usui T, et al. Transplantation of corneas reconstructed with cultured adult human corneal endothelial cells in nude rats. *Exp Eye Res*. 2004;79:231-237.
- Proulx S, Bensaoula T, Nada O, et al. Transplantation of a tissue-engineered corneal endothelium reconstructed on a devitalized carrier in the feline model. *Invest Ophthalmol Vis Sci*. 2009;50:2686-2694.
- Mimura T, Shimomura N, Usui T, et al. Magnetic attraction of iron-endocytosed corneal endothelial cells to Descemet's membrane. *Exp Eye Res*. 2003;76:745-751.
- Mimura T, Yamagami S, Usui T, et al. Long-term outcome of iron-endocytosing cultured corneal endothelial cell transplan-

- tation with magnetic attraction. *Exp Eye Res.* 2005;80:149-157.
29. Bartakova A, Kunzevitzky NJ, Goldberg JL. Regenerative cell therapy for corneal endothelium. *Curr Ophthalmol Rep.* 2014;2:81-90.
  30. Mimura T, Yamagami S, Usui T, Seiichi, Honda N, Amano S. Necessary prone position time for human corneal endothelial precursor transplantation in a rabbit endothelial deficiency model. *Curr Eye Res.* 2007;32:617-623.
  31. Mimura T, Yamagami S, Yokoo S, et al. Sphere therapy for corneal endothelium deficiency in a rabbit model. *Invest Ophthalmol Vis Sci.* 2005;46:3128-3135.
  32. Mimura T, Yokoo S, Araie M, Amano S, Yamagami S. Treatment of rabbit bullous keratopathy with precursors derived from cultured human corneal endothelium. *Invest Ophthalmol Vis Sci.* 2005;46:3637-3644.
  33. Okumura N, Kinoshita S, Koizumi N. Cell-based approach for treatment of corneal endothelial dysfunction. *Cornea.* 2014;33(suppl 11):S37-S41.
  34. Okumura N, Koizumi N, Ueno M, et al. ROCK inhibitor converts corneal endothelial cells into a phenotype capable of regenerating in vivo endothelial tissue. *Am J Pathol.* 2012;181:268-277.
  35. Frisco-Cabanos HL, Watanabe M, Okumura N, et al. Synthetic molecules that protect cells from anoikis and their use in cell transplantation. *Angew Chem Int Ed Engl.* 2014;53:11208-11213.
  36. Patel SV, Bachman LA, Hann CR, Bahler CK, Fautsch MP. Human corneal endothelial cell transplantation in a human ex vivo model. *Invest Ophthalmol Vis Sci.* 2009;50:2123-2131.
  37. Li S, Wang C, Dai Y, et al. The stimulatory effect of ROCK inhibitor on bovine corneal endothelial cells. *Tissue Cell.* 2013;45:387-396.
  38. Pipparelli A, Arsenijevic Y, Thuret G, Gain P, Nicolas M, Majo F. ROCK inhibitor enhances adhesion and wound healing of human corneal endothelial cells. *PLoS One.* 2013;8:e62095.
  39. Van Horn DL, Sendele DD, Seideman S, Bucu PJ. Regenerative capacity of the corneal endothelium in rabbit and cat. *Invest Ophthalmol Vis Sci.* 1977;16:597-613.
  40. Gospodarowicz D, Greenburg G, Alvarado J. Transplantation of cultured bovine corneal endothelial cells to species with nonregenerative endothelium. The cat as an experimental model. *Arch Ophthalmol.* 1979;97:2163-2169.
  41. Huang PT, Nelson LR, Bourne WM. The morphology and function of healing cat corneal endothelium. *Invest Ophthalmol Vis Sci.* 1989;30:1794-1801.
  42. Brunette I, Rosolen SG, Carrier M, et al. Comparison of the pig and feline models for full thickness corneal transplantation. *Vet Ophthalmol.* 2011;14:365-377.
  43. Bahn CF, Meyer RF, MacCallum DK, et al. Penetrating keratoplasty in the cat. A clinically applicable model. *Ophthalmology.* 1982;89:687-699.
  44. Ohno K, Mitooka K, Nelson LR, Hodge DO, Bourne WM. Keratocyte activation and apoptosis in transplanted human corneas in a xenograft model. *Invest Ophthalmol Vis Sci.* 2002;43:1025-1031.
  45. Ohno K, Nelson LR, Mitooka K, Bourne WM. Transplantation of cryopreserved human corneas in a xenograft model. *Cryobiology.* 2002;44:142-149.
  46. Proulx S, Audet C, Uwamaliya J, et al. Tissue engineering of feline corneal endothelium using a devitalized human cornea as carrier. *Tissue Eng Part A.* 2009;15:1709-1718.
  47. Heiligenhaus A, Steinmetz B, Lapuente R, et al. Recombinant tissue plasminogen activator in cases with fibrin formation after cataract surgery: a prospective randomised multicentre study. *Br J Ophthalmol.* 1998;82:810-815.
  48. Yoeruek E, Spitzer MS, Tatar O, et al. Toxic effects of recombinant tissue plasminogen activator on cultured human corneal endothelial cells. *Invest Ophthalmol Vis Sci.* 2008;49:1392-1397.
  49. Boulze Pankert M, Goyer B, Zaguia F, et al. Biocompatibility and functionality of a tissue-engineered living corneal stroma transplanted in the feline eye. *Invest Ophthalmol Vis Sci.* 2014;55:6908-6920.
  50. Jabs DA, Nussenblatt RB, Rosenbaum JT. Standardization of uveitis nomenclature for reporting clinical data. Results of the First International Workshop. *Am J Ophthalmol.* 2005;140:509-516.
  51. Taylor MJ, Hunt CJ. Dual staining of corneal endothelium with trypan blue and alizarin red S: importance of pH for the dye-lake reaction. *Br J Ophthalmol.* 1981;65:815-819.
  52. Matsuda M, Bourne WM. Long-term morphologic changes in the endothelium of transplanted corneas. *Arch Ophthalmol.* 1985;103:1343-1346.
  53. McCarey BE, Edelhauer HF, Lynn MJ. Review of corneal endothelial specular microscopy for FDA clinical trials of refractive procedures, surgical devices, and new intraocular drugs and solutions. *Cornea.* 2008;27:1-16.
  54. Merjava S, Neuwirth A, Mandys V, Jirsova K. Cytokeratins 8 and 18 in adult human corneal endothelium. *Exp Eye Res.* 2009;89:426-431.
  55. Riento K, Ridley AJ. Rocks: multifunctional kinases in cell behaviour. *Nat Rev Mol Cell Biol.* 2003;4:446-456.
  56. Bi YL, Zhou Q, Du F, Wu MF, Xu GT, Sui GQ. Regulation of functional corneal endothelial cells isolated from sphere colonies by Rho-associated protein kinase inhibitor. *Exp Ther Med.* 2013;5:433-437.
  57. Okumura N, Ueno M, Koizumi N, et al. Enhancement on primate corneal endothelial cell survival in vitro by a ROCK inhibitor. *Invest Ophthalmol Vis Sci.* 2009;50:3680-3687.
  58. Peh GS, Adnan K, George BL, et al. The effects of Rho-associated kinase inhibitor Y27632 on primary human corneal endothelial cells propagated using a dual media approach. *Sci Rep.* 2015;5:9167.
  59. Okumura N, Koizumi N, Ueno M, et al. Enhancement of corneal endothelium wound healing by Rho-associated kinase (ROCK) inhibitor eye drops. *Br J Ophthalmol.* 2011;95:1006-1009.
  60. Koizumi N, Okumura N, Ueno M, Nakagawa H, Hamuro J, Kinoshita S. Rho-associated kinase inhibitor eye drop treatment as a possible medical treatment for Fuchs corneal dystrophy. *Cornea.* 2013;32:1167-1170.
  61. Okumura N, Koizumi N, Kay EP, et al. The ROCK inhibitor eye drop accelerates corneal endothelium wound healing. *Invest Ophthalmol Vis Sci.* 2013;54:2493-2502.
  62. Ichijima H, Petroll WM, Barry PA, et al. Actin filament organization during endothelial wound healing in the rabbit cornea: comparison between transcorneal freeze and mechanical scrape injuries. *Invest Ophthalmol Vis Sci.* 1993;34:2803-2812.
  63. Kay ED, Cheung CC, Jester JV, Nimni ME, Smith RE. Type I collagen and fibronectin synthesis by retrocorneal fibrous membrane. *Invest Ophthalmol Vis Sci.* 1982;22:200-212.
  64. Petroll WM, Barry-Lane PA, Cavanagh HD, Jester JV. ZO-1 reorganization and myofibroblast transformation of corneal endothelial cells after freeze injury in the cat. *Exp Eye Res.* 1997;64:257-267.
  65. Sabet MD, Gordon SR. Ultrastructural immunocytochemical localization of fibronectin deposition during corneal endothelial wound repair. Evidence for cytoskeletal involvement. *Biol Cell.* 1989;65:171-179.
  66. Darby I, Skalli O, Gabbiani G. Alpha-smooth muscle actin is transiently expressed by myofibroblasts during experimental wound healing. *Lab Invest.* 1990;63:21-29.

67. Skalli O, Schurch W, Seemayer T, et al. Myofibroblasts from diverse pathologic settings are heterogeneous in their content of actin isoforms and intermediate filament proteins. *Lab Invest.* 1989;60:275-285.
68. Ljubimov AV, Burgeson RE, Butkowski RJ, et al. Extracellular matrix alterations in human corneas with bullous keratopathy. *Invest Ophthalmol Vis Sci.* 1996;37:997-1007.
69. Ishizaki M, Zhu G, Haseba T, Shafer SS, Kao WW. Expression of collagen I, smooth muscle alpha-actin, and vimentin during the healing of alkali-burned and lacerated corneas. *Invest Ophthalmol Vis Sci.* 1993;34:3320-3328.
70. Michels RG, Kenyon KR, Maumence AE. Retrocorneal fibrous membrane. *Invest Ophthalmol.* 1972;11:822-831.
71. Honda H, Ogita Y, Higuchi S, Kani K. Cell movements in a living mammalian tissue: long-term observation of individual cells in wounded corneal endothelia of cats. *J Morphol.* 1982; 174:25-39.
72. Petroll WM, Jester JV, Barry-Lane P, Cavanagh HD. Assessment of f-actin organization and apical-basal polarity during in vivo cat endothelial wound healing. *Invest Ophthalmol Vis Sci.* 1995;36:2492-2502.
73. Petroll WM, Ma L, Jester JV, Cavanagh HD, Bean J. Organization of junctional proteins in proliferating cat corneal endothelium during wound healing. *Cornea.* 2001;20:73-80.
74. Brown SI, Kitano S. Pathogenesis of the retrocorneal membrane. *Arch Ophthalmol.* 1966;75:518-525.
75. Jakobiec FA, Bhat P. Retrocorneal membranes: a comparative immunohistochemical analysis of keratocytic, endothelial, and epithelial origins. *Am J Ophthalmol.* 2010;150:230-242, e232.
76. Sherrard ES, Rycroft PV. Retrocorneal membranes. I. Their origin and structure. *Br J Ophthalmol.* 1967;51:379-386.
77. Miyamoto T, Sumioka T, Saika S. Endothelial mesenchymal transition: a therapeutic target in retrocorneal membrane. *Cornea.* 2010;29(suppl 1):S52-S56.
78. Petroll WM, Jester JV, Bean JJ, Cavanagh HD. Myofibroblast transformation of cat corneal endothelium by transforming growth factor-beta1, -beta2, and -beta3. *Invest Ophthalmol Vis Sci.* 1998;39:2018-2032.
79. Silbert AM, Baum JL. Origin of the retrocorneal membrane in the rabbit. *Arch Ophthalmol.* 1979;97:1141-1143.
80. Okumura N, Inoue R, Okazaki Y, et al. Effect of the Rho kinase inhibitor Y27632 on corneal endothelial wound healing. *Invest Ophthalmol Vis Sci.* 2015;56:6067-6074.